

The Lack of Structural and Dynamical Evolution of Elliptical Galaxies since $z \sim 1.5$: Clues from Self-Consistent Hydrodynamical Simulations

R. Domínguez-Tenreiro¹, J. Oñorbe¹, A. Sáiz^{1,2}, H. Artal¹ and A. Serna³

ABSTRACT

We present the results of a study on the evolution of the parameters that characterize the structure and dynamics of the relaxed elliptical-like objects (ELOs) identified at redshifts $z = 0, z = 1$ and $z = 1.5$ in a set of hydrodynamic, self-consistent simulations operating in the context of a concordance cosmological model. The values of the stellar mass $M_{\text{bo}}^{\text{star}}$, the stellar half-mass radius $r_{\text{e,bo}}^{\text{star}}$, and the mean square velocity for stars $\sigma_{3,\text{bo}}^{\text{star}}$, have been measured in each ELO and found to populate, at any z , a flattened ellipsoid close to a plane (the dynamical plane, DP). Our simulations indicate that, at the intermediate z 's considered, individual ELOs evolve, increasing their $M_{\text{bo}}^{\text{star}}$, $r_{\text{e,bo}}^{\text{star}}$, and $\sigma_{3,\text{bo}}^{\text{star}}$ parameters as a consequence of on-going mass assembly, but, nevertheless, their DP is roughly preserved within its scatter, in agreement with observations of the fundamental plane (FP) at different z 's. We briefly discuss how this lack of significant dynamical and structural evolution in ELO *samples* arises, in terms of the two different phases operating in the mass aggregation history of their dark matter halos. According to our simulations, most dissipation involved in ELO formation takes place at the early violent phase, causing the $M_{\text{bo}}^{\text{star}}$, $r_{\text{e,bo}}^{\text{star}}$, and $\sigma_{3,\text{bo}}^{\text{star}}$ parameters to settle down to the DP and, moreover, the transformation of most of the available gas into stars. In the subsequent slow phase, ELO stellar mass growth preferentially occurs through non-dissipative processes, so that the DP is preserved and the ELO star formation rate considerably decreases. These results hint, for the first time, at a possible way of explaining, in the context of cosmological simulations, different and apparently paradoxical observational results for elliptical galaxies.

Subject headings: dark matter— galaxies: elliptical and lenticular, cD— galaxies: formation— galaxies: evolution— galaxies: fundamental parameters— hydrodynamics

1. Introduction

Among all galaxy families, elliptical galaxies (E's) are the simplest ones and those that show the most precise regularities in the form of relations among some of their observable parameters.

¹Dpt. Física Teórica C-XI, Universidad Autónoma de Madrid, E-28049 Cantoblanco, Madrid, Spain; rosa.dominguez@uam.es; jose.onnorbe@uam.es; hector.artal@uam.es; ² Current address: Dept. of Physics, Mahidol University, Bangkok 10400, Thailand; alex@astro.phys.sc.chula.ac.th; ³Dpt. Física y A.C., Universidad Miguel Hernández, E-03206 Elche, Alicante, Spain; arturo.serna@umh.es

One of the most meaningful is the so-called fundamental plane relation (Djorgovski & Davis 1987; Dressler et al. 1987; Faber et al. 1987), defined by their observed effective radius, R_e^{light} , mean surface brightness within that radius, $\langle I^{\text{light}} \rangle_e$, and central line-of-sight velocity dispersion, $\sigma_{\text{los},0}$. Analyses of the Sloan digital sky survey (SDSS) sample of local elliptical galaxies confirm previous results on the FP, (see Bernardi et al. 2003a and references therein). Studies of the FP of early-type galaxies up to $z \sim 1$ (van Dokkum et al. 2001; van de Ven, van Dokkum, & Franx 2003; Wuyts et al. 2004; Treu et al. 2005) show that changes in the FP with z can be described in terms of the evolution of their average stellar mass-to-light ratio, M^{star}/L_B , as predicted by a scenario of pure luminosity evolution of their stellar populations, and with no further need for any significant structural or dynamical evolution of the sample (see, however, di Serego-Alighieri et al. 2005).

Different authors interpret the tilt of the FP relative to the virial relation as being caused by different assumptions concerning the dependence of the dynamical mass-to-light ratios, M_{vir}/L , or the mass structure coefficients, $c_M^{\text{vir}} = \frac{GM_{\text{vir}}}{3\sigma_{\text{los},0}^2 R_e^{\text{light}}}$, on the mass scale, see discussion in Oñorbe et al. (2005). A possibility is that M_{vir}/L grows systematically with increasing mass scale because the total dark-to-visible mass ratio, $M_{\text{vir}}/M^{\text{star}}$, grows (as suggested, e.g., by Ciotti, Lanzoni, & Renzini 1996; Pahre, Carvalho, & Djorgovski 1998; Cappellari et al. 2006). Otherwise, a dependence of c_M^{vir} on the mass scale could be caused by, among other possibilities, systematic differences in the relative spatial distribution of the baryonic and dark mass components of elliptical galaxies (Ciotti, Lanzoni, & Renzini 1996). Recently, we have confirmed these possibilities Oñorbe et al. (2005), finding that the samples of elliptical-like objects (ELOs) identified, at $z = 0$, in our fully-consistent cosmological hydrodynamical simulations exhibit just such trends giving rise to *dynamical* planes. They have also found that the physical origin of these trends presumably lies in the systematic decrease, with increasing ELO mass, of the relative amount of dissipation experienced by the baryonic mass component along ELO mass assembly. So, these results suggest that the dissipative processes involved in the mass assembly of elliptical galaxies result in the tilt of the FP relative to the virial plane. A consequence would be that the tilt of the FP must be preserved during those time intervals when no significant amounts of dissipation occur along E assembly.

Concerning the epochs of dissipation along elliptical assembly, because star formation (SF) requires gas cooling, the age distribution of the stellar populations of a given elliptical galaxy should reflect the time structure of the dissipative processes involved in its formation and assembly (i.e., when the dissipation rate was high, its time scale and so on). These age distributions indicate that, in E galaxies, most SF occurred (1), at high z , (2) on short timescales, and, moreover, (3) at higher z s and on shorter timescales for increasing E mass (they show age effects, see, e.g., Caldwell, Rose, & Concannon 2003; Bernardi et al. 2003b; Thomas et al. 2005). This would be the generic behavior of the dissipation rate history for elliptical galaxies, should the assumption on its connection with their SF rate history be correct.

Points 1 and 2 above are the basic ingredients of the so-called *monolithic collapse scenario*, see details and discussion in Peebles (2002); Matteucci (2003); Somerville et al. (2004). This scenario also explains another set of observational results on E homogeneity, such as, for example, (1), the

lack of significant structural and dynamical evolution of lens E galaxies, at least out to $z \sim 1$ (Treu & Koopmans 2004) (2), the lack of any strong structural evolution in the stellar mass-size relation since $z \sim 3$ (Trujillo et al. 2004; McIntosh et al. 2005) and (3), the confirmed existence of a population of old, relaxed, massive ($M^{\text{star}} > 10^{11} M_{\odot}$) spheroidal galaxies at intermediate redshifts ($z \sim 1 - 2$, Cimatti et al. 2002, 2004; Stanford et al. 2004) or even earlier (Mobasher et al. 2005). However, the monolithic scenario does not recover all the currently available observations on Es either. Important examples, suggesting that mergers at zs below $\sim 1.5 - 2$ could have played an important role in E assembly, are (1), the growth of the total stellar mass bound up in bright red galaxies by a factor of ~ 2 since $z = 1$ (Bell et al. 2004; Conselice, Blackburne, & Papovich 2005; Fontana et al. 2004; Drory et al. 2004; Bundy, Ellis, & Conselice 2005; Faber et al. 2005), implying that the mass assembly of most Es continues below $z = 1$, (2), the signatures of merging observed by the moment out to intermediate zs (Le Fèvre et al. 2000; Patton et al. 2002; Conselice 2003; Cassata et al. 2005), in particular of major dissipationless mergers between spheroidal galaxies (Bell et al. 2006), which translate into a relatively high merger rate for massive galaxies even below $z = 1$; and (3), the need for a young stellar component in some elliptical galaxies (van Dokkum & Ellis 2003; van der Wel et al. 2004) or, more particularly, the finding of blue cores (i.e., recent SF at the central regions) and inverse colour gradients in 30% - 40% of the spheroidal galaxies in some samples out to $z \sim 1.2$ (see Menanteau et al. 2004, and references therein).

The observational results above are paradoxical because they demand, on the one hand, that spheroids have passively-evolving stellar populations and an FP that preserves its tilt below $z \sim 1$ or higher and, on the other hand, that mass assembly is an on-going process for most of them and they still form some stars below these redshifts. In fact, one could think that, in principle, the tilt of the FP could be modified by these last processes, and so, the preservation of the FP tilt (or its evolution) is a very important issue because it could encode a lot of relevant information on the dissipation rate history of elliptical samples, and, consequently, on the physical processes underlying E formation and evolution. In order to reconcile all these physical assumptions and observational background within a formation scenario, it is useful to study E assembly from simple physical principles and in the context of the global cosmological model. Fully-consistent gravohydrodynamic simulations are a very convenient tool for working out this problem (Navarro & White 1994; Sommer-Larsen, Gotz, & Portinari 2003; Meza et al. 2003; Kobayashi 2005; Romeo et al. 2005). In fact, individual galaxy-like objects naturally appear as an output of the simulations, so that the parameters characterizing them can be measured and compared with observations. Concerning E assembly, the method has already proved to be useful. Apart from the physical origin of their FP (Oñorbe et al. 2005), the issue of age effects of their stellar populations has been addressed in Domínguez-Tenreiro, Sáiz, & Serna (2004), hereafter DSS04, where clues on how these age effects arise are given. Moreover, the structural and dynamical properties of these ELOs have been found to be consistent with observations (Sáiz, Domínguez-Tenreiro, & Serna 2004; Oñorbe et al. 2005). The next step is to study whether the dynamical FP of ELO samples does not evolve below $z \sim 1.5$ or so, and whether this is or is not consistent with on-going mass assembly as detected in real E samples, and if it is, to try to understand how this arises with regard to the cooling rate,

the SF rate and the mass assembly histories of ELOs. These are the issues addressed in this Letter.

2. The homogeneity of the elliptical population: clues from their assembly history

We have run five hydrodynamical simulations in the context of a concordance cosmological model (Spergel et al. 2003), in which the normalization parameter has been taken slightly high, $\sigma_8 = 1.18$, as compared with the average fluctuations of 2dFGRS or SDSS galaxies (Lahav et al. 2002; Tegmark et al. 2003) to mimic an active region of the universe (Evrard, Silk, & Szalay 1990). Galaxy-like objects of different morphologies form in these simulations. ELOs have been identified as those objects having a prominent, dynamically-relaxed stellar spheroidal component, with no disks and a very low cold-gas content. This stellar component has typical sizes of no more than $\sim 10 - 40$ kpc (hereafter the *baryonic object* or "bo" scale) and it is embedded in a halo of dark matter typically 10 times larger in size. ELOs also have an extended corona of hot diffuse gas. We consider the whole sample of ELOs identified in each of the five simulations at $z = 0$, $z = 1$, and $z = 1.5$ (samples E-Z0, E-Z1 and E-Z1.5, with 26, 24 and 16 ELOs, respectively) and analyze the evolution of their mass and velocity distributions between $z = 0$ and $z = 1.5$ by comparing the ELOs in these three samples. To run the simulations, we have used DEVA, a Lagrangian SPH-AP3M code using particles to sample dark matter or baryonic (i.e., gaseous and stellar) mass elements. We refer the reader to Serna, Domínguez-Tenreiro, & Sáiz (2003) for details on the simulation technique and to Sáiz, Domínguez-Tenreiro, & Serna (2004) for details on its implementation in the runs we analyze here and on the general sample properties at $z = 0$. All simulations started at a redshift $z_{\text{in}} = 20$. SF processes have been implemented, in the framework of the turbulent sequential SF scenario (Elmegreen 2002), through a simple parameterization that transforms cold locally-collapsing gas, denser than a threshold density, ρ_{thres} , into stars at a rate $d\rho_{\text{star}}/dt = c_*\rho_{\text{gas}}/t_g$, where t_g is a characteristic time-scale chosen to be equal to the maximum of the local gas-dynamical time and the local cooling time and c_* is the average SF efficiency at the scales resolved by the code. This is the empirical Kennicutt-Schmidt law (Kennicutt 1998). The five simulations share the same values for the SF parameters ($c_* = 0.3$ and $\rho_{\text{thres}} = 6.0 \times 10^{-25} \text{ gr cm}^{-3}$) and differ in the seed used to build up the initial conditions.

To characterize the structural and dynamical properties of ELOs, we will describe their three dimensional distributions of mass and velocity through the three intrinsic (i.e., three-dimensional) parameters (the stellar mass at the baryonic object scale, $M_{\text{bo}}^{\text{star}}$, the stellar half-mass radius at the same scale, $r_{\text{e,bo}}^{\text{star}}$, defined as that radius enclosing half the $M_{\text{bo}}^{\text{star}}$ mass, and the mean square velocity for stars, $\sigma_{3,\text{bo}}^{\text{star}}$) whose observational projected counterparts (the luminosity L , effective projected size $R_{\text{e}}^{\text{light}}$, and stellar central line of sight velocity dispersion, $\sigma_{\text{los,0}}$) enter the definition of the observed FP. We use three dimensional variables rather than projected ones to avoid projection effects. To measure the structural and dynamical evolution of ELOs, we carry out a principal component analysis of the E-Z0, E-Z1 and E-Z1.5 samples in the three dimensional variables $E \equiv \log M_{\text{bo}}^{\text{star}}$, $r \equiv \log r_{\text{e,bo}}^{\text{star}}$ and $v \equiv \log \sigma_{3,\text{bo}}^{\text{star}}$ through their 3×3 correlation matrix C . We have found

that one of the eigenvalues of C is, for the three ELO samples analyzed, considerably smaller than the others, so that at any z ELOs populate a flattened ellipsoid close to a two-dimensional plane in (E, r, v) space; the observed FP is the observational manifestation of this dynamical plane (DP). The eigenvectors of C indicate that the projection

$$E - \tilde{E}_z = \alpha_z^{3D}(r - \tilde{r}_z) + \beta_z^{3D}(v - \tilde{v}_z), \quad (1)$$

where \tilde{E}_z , \tilde{r}_z and \tilde{v}_z are the mean values of the variables E , r and v at redshift z , shows the DP viewed edge-on. Table 1 gives the planes eq. (1) for samples E-Z0, E-Z1 and E-Z1.5, as well as their corresponding thicknesses, $\sigma_{z,\text{Erv}}$, and the distances d_z of the point $(\tilde{E}_z, \tilde{r}_z, \tilde{v}_z)$ to the E-Z0 plane. We see that the sample averages \tilde{E}_z , \tilde{r}_z and \tilde{v}_z grow as z decreases, but in any case $|d_z| < \sigma_{z,\text{Erv}}$, so that they move *on* the E-Z0 plane within its rms scatter. Moreover, only 8.4 % and 0 % of ELOs in E-Z1 and E-Z1.5 samples respectively, are at distances greater than $\sigma_{z=0,\text{Erv}}$ from the E-Z0 plane. These results indicate that ELO evolution roughly preserves their DP. The results in Table 1 strongly suggest that the evolution shown by the FP of real elliptical galaxies is not the result of a dynamical or structural evolution of E samples, corroborating other observational findings on elliptical homogeneity (see §1). To try to understand these results, we report on ELO assembly and its effect on the DP preservation at intermediate and low redshift.

Our simulations indicate that ELOs are assembled out of mass elements that at high z are enclosed by those overdense regions R whose local coalescence length $L_c(t, R)$ (Vergassola et al. 1994) grows much faster than average, and whose mass scale, M_R (total mass enclosed by R) is on the order of an E total (i.e., including its halo) mass (see DSS04 and references therein). The virial mass of the ELO at low z , M_{vir} , is the sum of the masses of the particles that belong to R and are involved into the ELO merger tree. Analytical models, as well as N-body simulations indicate that two different phases operate along halo mass assembly: first, a violent fast one, in which the mass aggregation rates are high, and then, a slower one, with lower mass aggregation rates (Wechsler et al. 2002; Zhao et al. 2003; Salvador-Solé, Manrique, & Solanes 2005). Our hydrodynamic simulations give us, for each ELO, its mass aggregation track (i.e., its mass aggregation history along the main branch of the corresponding merger tree), and, moreover, its dissipation rate² and star formation rate histories, among others; these three histories are plotted in Figure 1 for a typical ELO. We have found that the fast phase occurs through a multiclump collapse following turnaround of the overdense regions, and it is characterized by fast head-on fusions experienced by the nodes of the cellular structure these regions enclose, resulting in strong shocks and high cooling rates for their gaseous component, and, at the same time, in strong and very fast star formation bursts (SFBs) that transform most of the available cold gas in R . For the massive ELOs in this work, this happens between $z \sim 6$ and $z \sim 2.5$ and corresponds to a cold mode of gas aggregation, as in Keres et al. (2005). Consequently, most of the dissipation involved in the mass assembly of a given ELO occurs

²That is, the amount of cooling per time unit experienced by those gas particles that at $z = 0$ form the ELO stellar component.

in this violent early phase at high z ; moreover, its rate history is reflected by the SF rate history, as illustrated in Figure 1. This implies that the dynamical variables settle down to the ELO DP at this early phase. This plane is tilted relative to the virial plane as discussed in §1 see Oñorbe et al. (2005) and also Robertson et al. (2005) for pre-prepared mergers.

The slow phase comes after the multiclump collapse. In this phase, the halo mass aggregation rate is low and the M_{vir} increment results from major mergers, minor mergers or continuous accretion. Our cosmological simulations show that the fusion rates are generally low, and that a strong SFB follows a major merger only if enough gas is still available after the early violent phase. This is very unlikely in any case, and it becomes more and more unlikely as M_{vir} increases (see DSS04). And so, these mergers imply only a modest amount of energy dissipation or SF, as the major merger in Figure 1 at $t/t_U \sim 0.66$ (where t_U is the age of the universe) illustrates. Note, however, that mergers play an important role in this slow phase: $\sim 50\%$ of ELOs in the sample have experienced a major merger event at $2 < z < 0$, which results in the increase of the ELO mass content (see Fig. 1), size r , and stellar mean square velocity v . A consequence of the lack of dissipation could be that the DP is preserved at the slow phase, and in fact, we have found in our cosmological simulations that *dissipationless* merger events roughly preserve it see Table 1 ³.

Apart from ELO stellar mass growth following dissipationless mergers in the slow phase, our simulations indicate that $M_{\text{bo}}^{\text{star}}$ can also increase as a consequence of newborn stars, formed either (1), within the ELO itself from accreted gas or gas coming in satellites, that falls to the central regions before being turned into stars (see the weak SFBs in Fig. 1 at $0.45 < t/t_U < 0.68$) or (2) through mergers, as the SB at $t/t_U \sim 0.68$ in Figure 1. While the first implies quiescent modes of star formation (see Papovich et al. 2005) and could explain the blue cores observed in some relaxed spheroids, both could explain the need for a young stellar population to fit some E spectra (see references above). Major merger events become less frequent as time elapses, allowing for a higher fraction of relaxed spheroids. Both, on-going stellar mass assembly (either through stellar mass aggregation or forming newborn stars) and the decrease of the major merger rate, imply an increase of the stellar mass density contributed by relaxed ELOs. In fact, we find that it has changed by a factor of 2.1 between $z = 1$ and $z = 0$, consistent with empirical estimations (see §1).

To sum up, the main result we report on is the homogeneity of the relaxed ELO population with respect to z , as measured through the dynamical plane defined by their stellar masses, three-dimensional sizes and mean square stellar velocities at different z s, and, at the same time, the increase of the average values of these parameters as time elapses. The simulations also provide us with clues to how these evolutionary patterns arise from the physical processes involved in E formation, namely, the plane’s appearance at an early violent phase as a consequence of E assembly out of gaseous material, with cooling and on short timescales (as in the monolithic collapse scenario),

³The preservation of the FP in pre-prepared dissipationless mergers has already been studied by Capelato, Carvalho, & Calberg (1995); González-García & van Albada (2003); Nipoti, Londrillo, & Ciotti (2003) and Boylan-Kolchin, Ma, & Quataert (2005).

and the plane’s preservation during a later, slower phase, where dissipationless merging plays an important role in stellar mass assembly (as in the hierarchical scenario of E formation). This early gas consumption of proto-ellipticals also explains why most of the stars of today elliptical galaxies formed at high redshifts, while they are assembled later on (see de Lucia et al. 2006, for similar conclusions from a semi-analytic model of galaxy formation grafted to the *Millennium Simulation*). Simulations also provide clues to why E homogeneity is consistent with the appearance of blue cores as well as with the increase of the stellar mass contributed by the E population as z decreases. We conclude that the simulations provide a unified scenario within which most current observations on elliptical galaxies can be interrelated. This scenario shares some characteristics with previously proposed scenarios, but it also has significant differences, mainly that stars form out of cold gas that had never been shock heated at the halo virial temperature and then formed a disk, as the conventional recipe for galaxy formation propounds (see discussion in Binney 2004; Keres et al. 2005, and references therein). To finish, let us note that the scenario for elliptical galaxy formation emerging from our simulations has the advantage that their dark mass and gas aggregation histories result from simple physical laws acting on generic initial conditions (i.e., realizations of power spectra consistent with CMB anisotropy data).

This work was partially supported by the MECD (Spain) through grants AYA-07468-C03-02 and AYA-07468-C03-03 from the Plan Nacional de Astronomía y Astrofísica. We thank E. Salvador-Sol for discussions, and the Centro de Computación Científica (UAM) for computing facilities. A.S. thanks the European Union for Fonds Européens de Développement Régional (FEDER) financial support.

REFERENCES

Bell, E.F., et al. 2004, ApJ, 608, 752

Bell, E.F., et al. 2006, ApJ, in press (astro-ph/0506425 preprint)

Bernardi, M., et al. 2003a, AJ, 125, 1866

Bernardi, M., et al. 2003b, AJ, 125, 1882

Binney, J. 2004, MNRAS, 347, 1093

Boylan-Kolchin, M., Ma, C.-P., & Quataert, E. 2005, MNRAS, submitted (astro-ph/0502495)

Bundy, K., Ellis, R.S., & Conselice, C.J. 2005, ApJ, 625, 621

Cassata, P., et al. 2005, MNRAS, 357, 903

Caldwell, N., Rose, J.A., & Concannon, K.D., 2003, AJ, 125, 2891

Capelato, H.V., de Carvalho, R.R., & Calberg, R.G. 1995, ApJ, 451, 525

Cappellari, M., et al. 2006, MNRAS, in press (astro-ph/0505042 preprint)

Cimatti, A., et al. 2002, A&A, 381, L68

Cimatti, A., et al. 2004, Nature, 430, 184

Ciotti, L., Lanzoni, B., & Renzini, A. 1996, MNRAS, 282, 1

Conselice, C.J. 2003, ApJS, 147, 1

Conselice, C.J., Blackburne, J.A., & Papovich, C. 2005, ApJ, 620, 564

de Lucia, G., Springel, V., White, S.D.M., Croton, D., & Kauffmann, G. 2006, MNRAS, in press (astro-ph/0509725 preprint)

di Serego Alighieri et al. 2005, astro-ph/0506655 preprint

Djorgovski, S., & Davis, M. 1987, ApJ, 313, 59

Domínguez-Tenreiro, R., Sáiz, A., & Serna, A. 2004, ApJ, 611L, 5 (DSS04)

Dressler, A., Lynden-Bell, D., Burstein, D., Davies, R.L., Faber, S.M., Terlevich, R., & Wegner, G. 1987, ApJ, 313, 42

Drory, N., Bender, R., Feulner, G., Hopp, U., Maraston, C., Snigula, J., & Hill, G.J. 2004, ApJ, 608, 742

Elmegreen, B. 2002, ApJ, 577, 206

Evrard, A., Silk, J., & Szalay, A.S. 1990, ApJ, 365, 13

Faber, S.F., Dressler, A., Davies, R.L., Burstein, D., Lynden-Bell, D., Terlevich, R., & Wegner, G. (1987), in *Nearly Normal Galaxies: From the Planck Time to the Present*, ed. S.M. Faber (New York: Springer), 175

Faber, S.M., et al. 2005, ApJ, submitted (astro-ph/0506044 preprint)

Fontana, A., et al. 2004, A&A, 424, 23

González-García, A.C., & van Albada, T.S. 2003, MNRAS, 342, 36

Keres, D., Katz, N., Weinberg, D., & Davé, R. 2005, astro-ph/0407095 preprint

Kennicutt, R. 1998, ApJ, 498, 541

Kobayashi, C. 2005, astro-ph/0506094 preprint

Lahav, O., et al. 2002, MNRAS, 333, 961L

Le Fèvre, O., et al. 2000, MNRAS, 311, 565

Matteucci, F. 2003, *Ap&SS*, 284, 539

McIntosh, D.H., et al. 2005, *ApJ*, in press (astro-ph/0411772)

Menanteau, F., et al. 2004, *ApJ*, 612, 202

Meza, A., Navarro, J., Steinmetz, M., & Eke, V.R., 2003, *ApJ*, 590, 619

Mobasher, B., et al. 2005, astro-ph/0509768 preprint

Navarro, J.F., & White, S.D.M., 1994, *MNRAS*, 267, 401

Nipoti, C., Londrillo, P., & Ciotti, L. 2003, *MNRAS*, 342, 501

Oñorbe, J., Domínguez-Tenreiro, R., Sáiz, A., Serna, A., & Artal, H. 2005, *ApJ Letters*, 632, 570

Pahre, M.A., de Carvalho, R.R., & Djorgovski, S.G. 1998, *AJ*, 116, 1606

Papovich, C., et al. 2005, astro-ph/0501088 preprint

Patton, D.R, et al. 2002, *ApJ*, 565, 208

Peebles, P.J.E. 2002, in *A New Era in Cosmology*, ASP Conf., eds. N. Metcalf and T. Shanks

Robertson, B., Cox, T.J., Hernquist, L., Franx, M., Hopkins, P.F., Martini, P. and Springel, V. 2005, *ApJ*, submitted (astro-ph/0511053 preprint)

Romeo, A.D., PortinariL. & Sommer-Larsen, J. 2005, *MNRAS*, 361, 983

Sáiz, A., Domínguez-Tenreiro, R., & Serna, A. 2004, *ApJ*, 601, L131

Salvador-Solé, E., Manrique, A., & Solanes, J.M. 2005, *MNRAS*, 358, 901

Serna, A., Domínguez-Tenreiro, R., & Sáiz, A. 2003, *ApJ*, 597, 878

Sommer-Larsen, J., Gotz, M., & Portinari, L. 2003, *ApJ*, 596, 47

Somerville, R.S., et al. 2004, *ApJ Letters* 600, 135

Spergel, D.N., et al. 2003, *ApJS*, 148, 175

Stanford, S.A., et al., 2004, *AJ*, 127, 131

Tegmark, M., et al. 2003, *Phys. Rev. D* 69, 103501

Thomas, D., Maraston, C., Bender, R. & Mendes de Oliveira, C. 2005, *ApJ*, 621, 673

Treu, T. & Koopmans, L.V.E. 2004, *ApJ*, 611, 739

Treu, T., et al. 2005, astro-ph/0503164 preprint

Trujillo, I., et al. 2004, *ApJ*, 604, 621

van de Ven, G., van Dokkum, P.G. & Franx, M. 2003, *MNRAS*, 344, 924

van der Wel, A., Franx, M., van Dokkum, P.G., & Rix, H.-V. 2004, *ApJ Letters*, 601, L5

van Dokkum, P. G., Franx, M., Kelson, D. D., & Illingworth, G. D. 2001, *ApJ*, 553, L39

van Dokkum, P.G., & Ellis, R.S. 2003, *ApJ*, 592, L53

Vergassola, M., Dubrulle, B., Frisch, U. & Noullez, A. 1994, *A&A*, 289, 325

Wechsler, R.H., Bullock, J.S., Primack, J.R., Kravtsov, A.V. & Dekel, A. 2002, *ApJ*, 568, 52

Wuyts, S., van Dokkum, P.G., Kelson, D.D., Franx, M., Illingworth, G.D., 2004, *ApJ*, 605, 677

Zhao, D.H., Mo, H.J., Jing, Y.P., & Börner, G. 2003, *MNRAS*, 339, 12

Table 1:

Sample	\bar{E}_z	\bar{r}_z	\bar{v}_z	α_z^{3D}	β_z^{3D}	$\sigma_{z,Erv}$	d_z
E-Z0	11.0	0.75	2.34	0.43	2.07	.011	
E-Z1	10.8	0.52	2.30	0.25	2.10	.011	.008
E-Z1.5	10.9	0.49	2.33	0.31	2.01	.013	.009

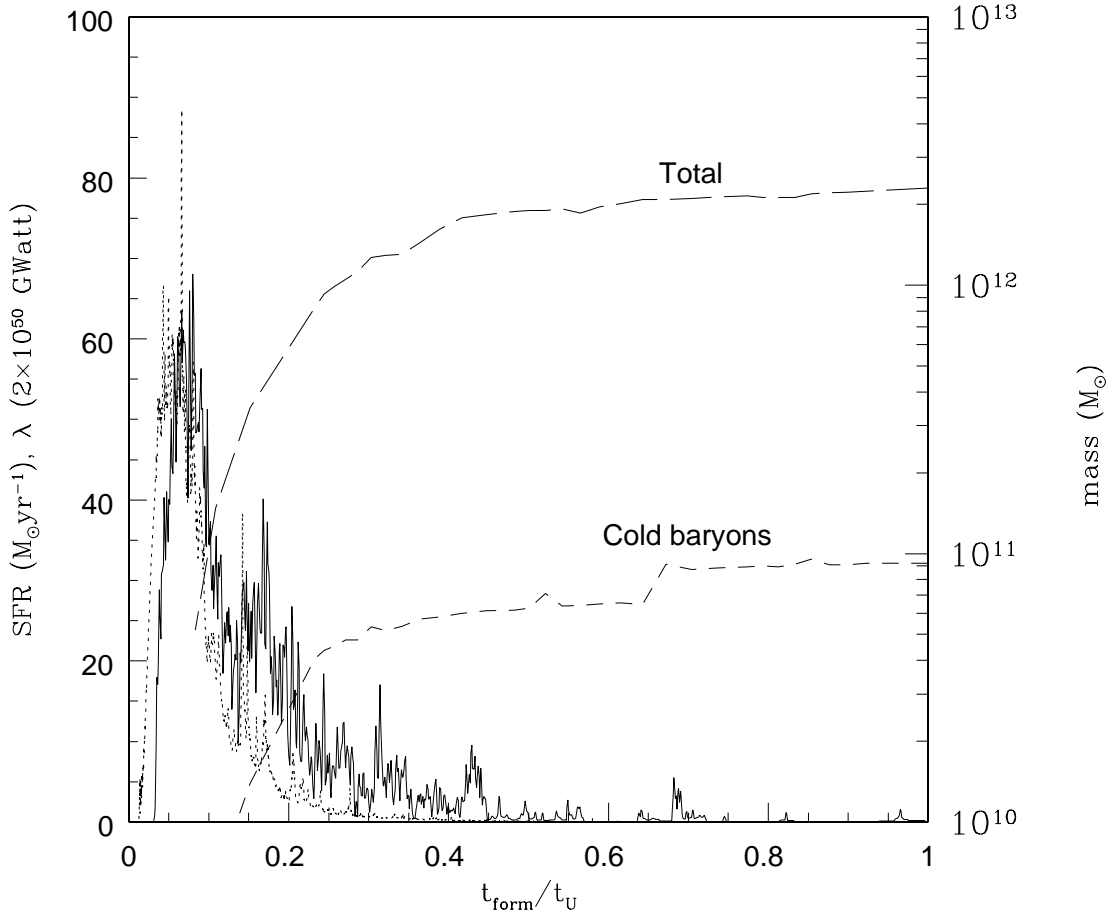


Fig. 1.— Cooling rate history λ (dotted line) and the star formation rate history (solid line) of a typical ELO in the simulations. We also plot its mass aggregation tracks, both for cold baryons (i.e., stars and cold gas) and total mass. The fast (left) and slow (right) phases of mass aggregation are clearly shown.